

Using Earthquake Data to Map Faults in 3-D with Gocad: Examples at Different Scales

Sara Carena

Dept. für Geo- und Umweltwissenschaften, Sektion Geologie, Luisenstr. 37, 80333 München, Germany. Email: scarena@geophysik.uni-muenchen.de.

Eine Reihe neuer Techniken zur 3-D Kartierung von Störungen wurde entwickelt, deren Anwendung von Modellen einzelner Störungsoberflächen oder kleiner Gruppen von Störungen bis hin zu regionalen tektonischen Modellierung reicht. Ein Beispiel zur Anwendung dieser Techniken an einzelnen, kleinen Strukturen, ist die Northridge Überschiebung in der westlichen Transverse Ranges von Südkalifornien. Die 3-D Geometrie der Störung, die das M 6.8 1994 Northridge Erdbeben erzeugte, wurde durch Nachbeben bestimmt. Auch größere Störungssysteme können modelliert werden. Ein Beispiel hierfür ist das San Andreas Störung System nahe des San Gorgonio Passes in der östlichen Transverse Ranges von Südkalifornien. Eine Studie der 3-D Krustenstruktur im zentralen Taiwan ist ein Beispiel für die Modellierung regionaler Tektonik und Gebirgsbildung. Zum ersten Mal wurde hier die große Sohlfläche unter Taiwan abgebildet.

Several new techniques in 3-D fault mapping have been developed, whose applications range from models of single fault surfaces or small fault networks, to regional tectonic models. An example of how these techniques can be applied to single structures is that of the Northridge thrust, western Transverse Ranges, southern California. The 3-D geometry of the fault that generated the M 6.8, 1994 Northridge earthquake was determined from the aftershocks of this event. Larger fault systems can be modeled too. An example of this is the San Andreas fault system near San Gorgonio Pass, eastern Transverse Ranges, southern California. A study of the 3-D structure of the crust in central Taiwan is instead an example of modeling applied to regional tectonics, and mountain building in particular. For the first time the large detachment beneath Taiwan was imaged.

1 Earthquake data and 3-D Fault Mapping

1.1 Introduction

Traditionally, the problem of determining the detailed 3-D geometry of active faults has been addressed either by collecting geological and structural information at the surface of the Earth and extrapolating the geometry at depth using various theories and assumptions, or by direct imaging with seismic reflection techniques and wells, as it is routinely done in oil exploration. Earthquake data are often an under-utilized source of information concerning 3-D fault geometry. SHAW & SHEARER (1999) and SHAW ET AL. (2002) showed the benefits of combining earthquake data with seismic reflection data in 3-D fault modeling and in better defining regional earthquake hazards. Hopefully, this kind of approach will become more common.

1.2 Main Issues: Earthquake Size, Aftershocks, Location Quality, Focal Plane Solutions

Hypocenter locations and focal mechanisms can provide direct information about the geometry of active faults at depths far greater than any other method. There are several key issues however that need to be addressed before using earthquake data to model fault geometry, namely earthquake size, density and distribution of earthquakes on faults, and data quality.

In seismology, large earthquakes have often been the preferred means of finding out the orientation of the fault plane, by determining the earthquake focal solution. This approach usually results in fault geometries that are exceedingly simple, when not outright wrong. For example, early models of the Chelungpu thrust in Taiwan (e.g. LEE & MA 2000, KIKUCHI ET AL. 2000) that show a uniform 30°

dipping plane to depths of 20 km are incorrect, because they assume that the fault keeps a constant strike and dip with increasing depth. In this case however the shallow main-shock focal mechanism is not representative of the entire geometrically complex fault, which flattens to a sub-horizontal detachment at 5-6 km depth (YUE ET AL. 2005). In other instances, the slip direction in a large earthquake does not coincide with the long-term slip direction (see the Northridge thrust, CARENA & SUPPE 2002).

Often most aftershocks are not located on the main fault that ruptured, but on nearby ones (LIU ET AL. 2003). Ambiguities could be avoided by imaging the entire fault network in the area using background seismicity and previous earthquake sequences. This approach can help us to recognize the principal plane by matching it with previous events with similar focal mechanisms. Microearthquakes ($M \leq 3$) are particularly useful for this purpose due to their abundance. Networks that can reliably record microseismicity already exist in a few regions of the world, and more are being added.

The most important issue to consider is the quality of the earthquake data. In recent years, several authors have developed new methods of improving earthquake hypocenter locations significantly (GOT ET AL. 1994, JONES & STEWART 1997, RUBIN ET AL. 1999, NICHOLSON ET AL. 2000; RICHARDS-DINGER & SHEARER 2000, WALDHAUSER & ELLSWORTH 2002). In our work we gave preference to the clustering method of JONES & STEWART (1997) because it can be quickly applied to large earthquake catalogs (hundreds of thousands of events), because the only information needed about the earthquakes are their location and location uncertainties, and because it does not result in the exclusion of some events. Of course, the more details we want to extract about the fault 3-D geometry, the more a need arises for combining different methods in order to get the best possible hypocenter locations. In fact, even when using the clustering method, the ideal approach is to start with an earthquake catalog that has already been relocated to minimize systematic errors as much as possible (JONES & STEWART 1997).

Focal mechanisms are extremely useful in 3-D fault modeling because, besides providing confirmation of fault geometry when there is an abundance of hypocenter locations, in certain cases they provide enough additional information to image even faults with a small number of events on them. Unlike event locations, that only provide information about fault shape, focal mechanisms allow us to determine fault type and direction of motion. Thus we fitted fault surfaces simultaneously to both earthquake hypocenter locations and principal planes extracted from focal mechanisms whenever possible. The main problem with focal mechanisms is their reliability, which decreases with decreasing earthquake size, as the event is recorded only at a few stations.

1.3 Integration of Other Data Types

Earthquakes are not the only kind of data that can be successfully used in 3-D fault modeling, and earthquakes do not occur everywhere. Therefore other types of data should be integrated in the model whenever available to fill any gaps and to better constrain it. SHAW & SHEARER (1999) and SHAW ET AL. (2002), for instance, have shown how combining seismic reflection profiles with relocated earthquake data can significantly improve results when imaging blind faults.

Surface geological data, like strike and dip measurements, stratigraphy, and the detailed location of fault traces and earthquake surface breaks are also key data, because seldom large numbers of earthquakes occur at depths shallower than a few kilometers. For example, the aftershocks of the Northridge earthquake occurred mostly below 3-5 km depth and did not provide any information about fault geometry, or even the presence of any faulting, at shallower depths (CARENA & SUPPE 2002). In the case of the Chelungpu thrust in Taiwan, very few aftershocks of the 1999 Chi-Chi earthquake occurred on the thrust itself; most of them were deeper and occurred on nearby faults. Nevertheless, YUE ET AL. (2005) were able to generate a detailed 3-D fault model on the basis of strike and dip data, integrating them with surface breaks and several seismic profiles, and then connecting their model with the deeper fault network imaged from seismicity.

Digital elevation models are necessary to transform a map of fault traces or surface breaks into a 3-D trace that can be directly incorporated into the fault model. Fault depth measurements in wells are also a very good constraint when available, as they are yet another type of data that can give us information about fault geometry at shallow depths.

1.4 Some Techniques in 3-D Surface Building

Realistic fault geometry is first of all a geometry that allows the fault to slip. Large jogs perpendicular to the long-term slip direction and large bumps are unrealistic, because not only they would impede slip itself, but also because slip on the fault would quickly destroy them. On the other hand, corrugations parallel to the slip direction can certainly exist and have been used by some authors to constrain the 3-D fault geometry when modeling faults. Based on faults whose geometry is well known due to direct observation of the fault surface or to numerous wells intersecting it, THIBAUT ET AL. (1996) developed the concept of faults as “thread surfaces”. They improve the results of interpolating between scattered points (a common characteristic of fault data) by assuming that faults behave in a way similar to a nut-and-bolt system, with the contact surface between the two blocks dented by grooves (threads) produced by slip on the fault. They obtain the orientation of the threads (which are lineations on the fault plane at any scale, from striae visible in the field, to corrugations of the fault surface with wavelengths up to 10 km or greater) from areas with denser data, and apply their thread criterion to the interpolation in areas of low data density, thus obtaining a consistent fault geometry everywhere. A similar approach is that of MALLET ET AL. (1999) and MALLET (2002), who show how fault corrugations imaged from actual data can be combined with the assumption that long-term slip must occur parallel to the corrugations to further improve a 3-D fault model, removing bumps on the surface that would impede slip and which are most likely the result of scattering or gaps in the data.

2 A New Approach to 3-D Fault Mapping

Our approach requires handling up to several hundred thousands of earthquakes at once, and the ability to integrate different data types into a single model. This is why Gocad was chosen as a modeling toolbox. While the main focus of Gocad is geomodeling, it was not designed specifically with handling earthquakes in mind, so we had to devise some procedures to be able to use it to manipulate earthquake data efficiently.

We start from hypocenter locations that have been relocated if possible. The hypocenter locations are then clustered using the clustering method developed and described by JONES & STEWART (1997) and modified by NICHOLSON ET AL. (2000). Clustering results in tighter earthquake distributions (a “sharper” image, see fig. 1), which makes the process of selecting subsets of earthquakes much easier.

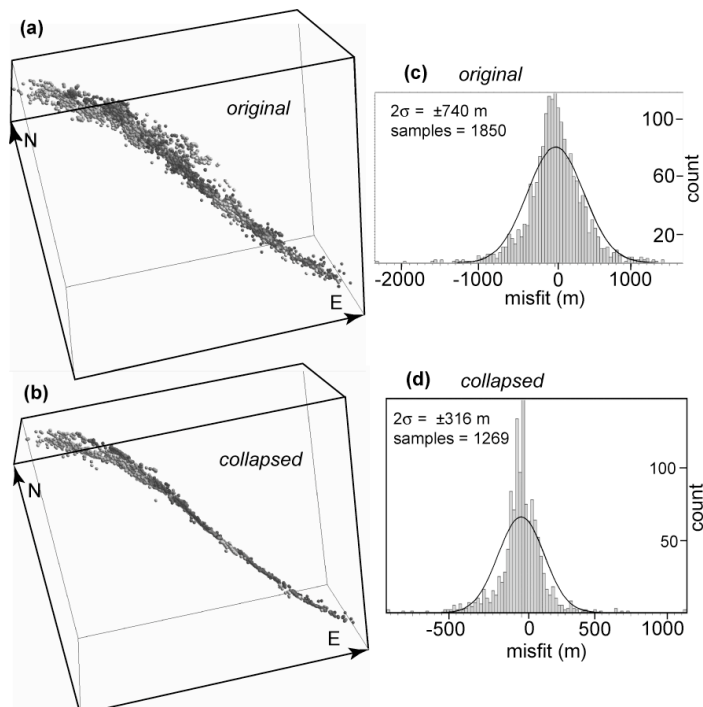


Fig. 1. Example of earthquake hypocenters (aftershocks of M 7.1, 1986, Loma Prieta, California, earthquake) before (a) and after (b) application of the clustering algorithm. (c) and (d) show the misfit to the 3-D fault surface.

Fault geometry can be constrained by focal mechanisms as well. The comparison between earthquake hypocenter distribution and focal mechanisms in 3-D allows us to [1] distinguish between principal and auxiliary nodal planes, thus making it possible to select only the principal planes and vectors in the data set, [2] identify and map faults which have only a few events associated with them, [3] determine the current slip direction on faults. Nodal planes and slip vectors are imported into Gocad as surfaces and lines. Once one of the two nodal planes has been identified as the principal plane, focal mechanisms can then be transformed into point sets and used directly in fault surface building.

A third type of constraint that can be applied to fault geometry is surface traces, either in the form of known breaks caused by a specific earthquake (CARENA & SUPPE 2002), or as mapped fault traces. Surface traces constrain the position of the top of the fault and may disclose a near-surface change in fault dip that could have gone undetected due to the general lack of earthquakes at shallow depths.

Once earthquake hypocenter locations have been relocated and/or clustered, and all the other data types have been transformed into a suitable format, we separate clusters of earthquake hypocenters that illuminate different faults. This is the most subjective part of the procedure, as it has to be done manually, but in most cases the clusters are fairly obvious features when viewed in 3-D. Different operators performing the selection could include or exclude a few different hypocenters, but in the majority of cases where there is a recognizable cluster, these differences are limited to the outer edges of the cluster. Because the steps that follow the selection always include some form of averaging of the hypocenter locations, small differences in the initial selection of hypocenters will not have any appreciable influence on the final fault geometry.

Occasionally, it is not possible to separate clusters adequately because they intersect forming X- or complex junctions. In such cases only better earthquake locations might solve the problem, or at least reduce uncertainties (for example, once earthquakes are relocated, an X-junction might turn out to have one through-going fault, and one slightly offset fault). At other times, faults come together in T- or Y- junctions. The earthquake clusters can usually be separated at such junctions, but there will be uncertainty as to where exactly the truncated fault stops. Also, at the junction earthquake density is often higher and there can be more scattering than far from it, thus when separating the clusters many earthquakes of the truncated fault might be included in the through-going fault cluster. Situations where T- and Y- junctions exist can of course be improved too by better relocation of the earthquakes. Another kind of useful information in separating these types of clusters is their timing: if the two faults are active in different periods of time, then the clusters can be separated by accounting for both position and timing of the events.

As previously mentioned, any other data points relative to fault position should also be considered, for example the depth of a fault in oil wells, or seismic lines on which a fault has been identified (for an excellent example, see SHAW & SHEARER 1999, and SHAW ET AL. 2002). These additional data types are especially important: they are usually available for depths up to a few km below the surface, but this is precisely the depth range where often very few earthquakes occur, and allow us to image the shallow geometry of the fault.

For each fault, all different types of data should be merged so that they can be used simultaneously to build a first approximation of the fault surface. In our case we transform all data into sets of points. We choose points as our basic data type because the majority of our data are earthquake hypocenter locations, which are already discrete points. We then build our surfaces directly from the set of points, setting constraints as needed and then smoothing the resulting surface with the Gocad Discrete Smooth Interpolator (DSI, MALLET 2002). Several iterations of the DSI are usually necessary before all the irregularities in the surface that have a size below the minimum resolution of the data are smoothed out.

2 Applications and Results

We have applied the techniques described above to several cases at different scales and in different tectonic settings, and three of these are briefly described below: [1] a thrust fault associated with a restraining bend (Northridge thrust, southern California), [2] a network of strike-slip and thrust faults (San Andreas fault and surrounding faults near San Gorgonio Pass, southern California), and [3] an entire orogen in a subduction margin setting (Taiwan).

2.1 Northridge Thrust, Southern California

The aftershocks of the 1994 Northridge earthquake (M 6.8) illuminate the structure beneath the San Fernando Valley (northwestern Los Angeles) in 3-D. We combined aftershocks and geological data to build an image of the 3-D geometry of the north-vergent Northridge blind thrust to a depth of 21 km. The most striking feature of the imaged fault is mega-corrugations oriented parallel to the mean aftershock slip vector, with most of the 1994 slip confined to west of the largest corrugation (lateral ramp, fig. 2). We also imaged the partially overlying south-vergent San Fernando thrust, which broke to the surface in a complex rupture in 1971 (M 7.1). Both thrusts produce fault-related folding because of either fault propagation or fault bends (SUPPE 1983). This deeper folding however is masked by overlying complex deformation in the cover, which is one reason why the Northridge thrust was not identified until it ruptured in 1994. We used trishear fold modeling (ERSLEV 1991) based on our 3-D fault geometry to evaluate possible folding due to slip on the Northridge thrust as well as its interaction with the overlapping San Fernando thrust and with shallow structures in the cover. This example illustrates the importance of earthquake data to structural geology and the value of its 3-D integration with surface and near-surface geological data.

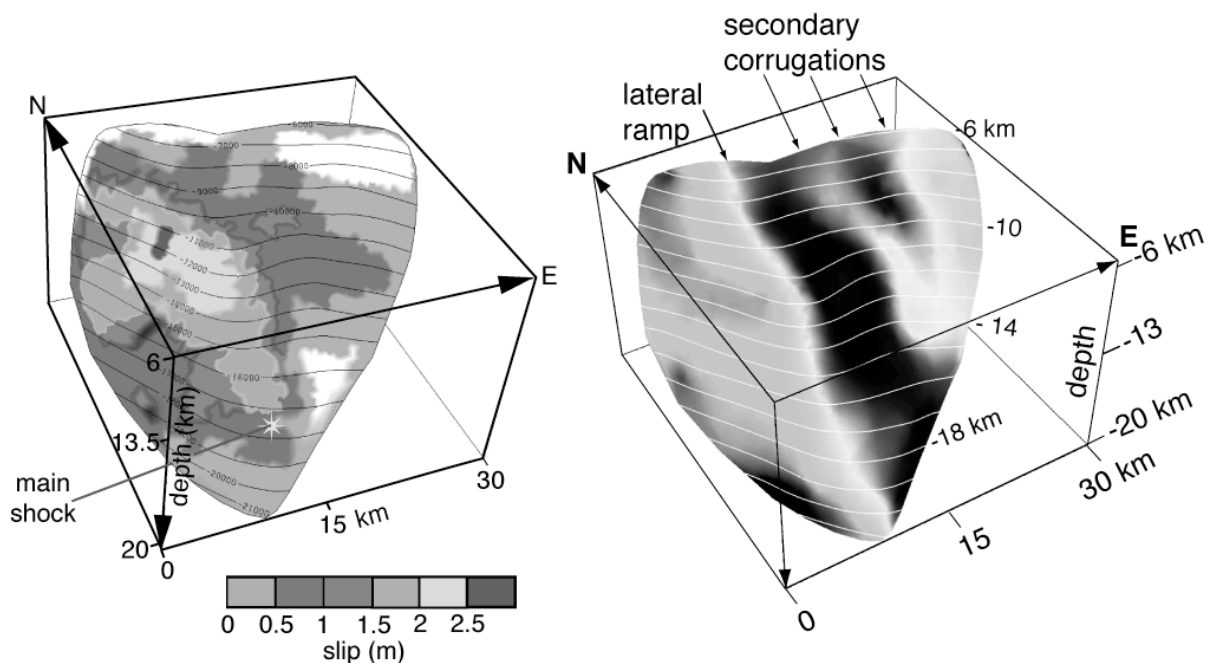


Fig. 2. 3-D model of the Northridge thrust. Coseismic slip distribution shown on the left, fault corrugations indicated on the right.

2.2 San Andreas Fault Near San Gorgonio Pass, Southern California

The 1200 km long San Andreas fault (SAF) loses its apparent continuity in southern California near San Gorgonio Pass (ALLEN 1957). This fact raises significant questions, given the dominant role of this fault in active California tectonics. What is the fundamental 3-D geometry and kinematics of the San Andreas fault system in this complex region? Is a through-going, San Andreas rupture from the Mojave desert to the Coachella valley possible? We explored the issue of 3-D continuity by mapping over 60 faults in this region to depths of 15-20 km from hypocenter locations and focal mechanisms. We were able to constrain the 3-D geometry of the SAF near San Gorgonio Pass from the 3-D geometry of the fault network surrounding it, as the San Andreas itself appears to be aseismic here. The most likely configuration is for the San Andreas fault to merge into the shallow-dipping San Gorgonio Pass thrust northwest of Indio (fig. 3). We concluded that there is no direct continuity at present, but rather a network of faults, and the only kind of rupture possible for the SAF in this region is a complex rupture, involving both strike-slip and reverse faulting. GPS measurements also suggest that, despite the fact large motions must have occurred in the past, only minor ones are occurring today in this area (YULE & SIEH 2001, MEADE ET AL. 2002, YULE & SIEH 2003). Applying our findings about the fault geometry, we explored several simple earthquake scenarios, following KING ET AL. (1994), to

determine the most favorable conditions for a through-going rupture of the San Andreas fault system from the Mojave desert to the Coachella valley (CARENA ET AL. 2004).

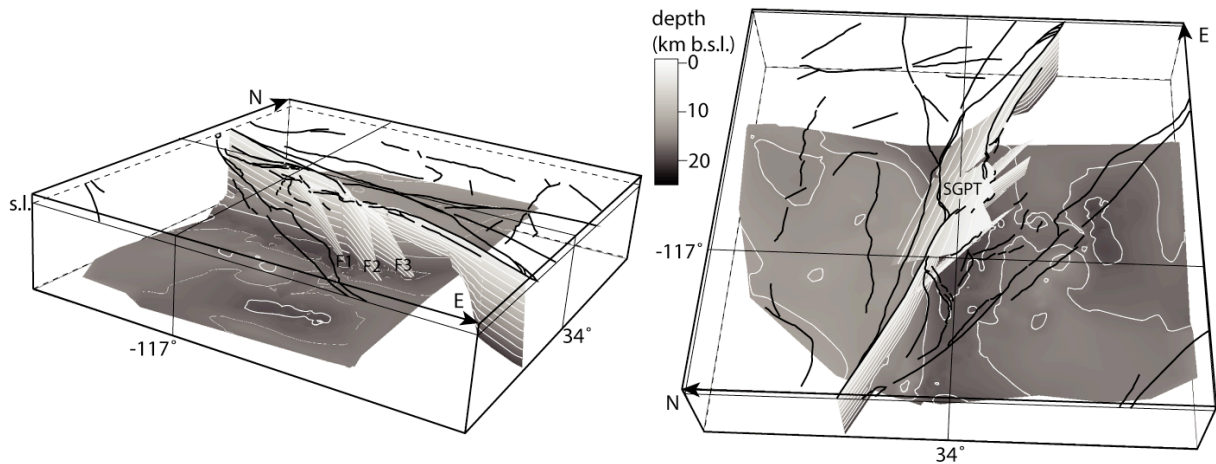


Fig. 3. Two different views of the detailed 3-D geometry of the San Andreas fault system between Cajon Pass and Indio. SGPT=San Gorgonio Pass thrust. F1, F2, F3 are tear faults. The gray surface below the faults represents the base of the seismogenic crust in this region.

2.3 Taiwan Orogen

Active deformation in the upper crust beneath central Taiwan is illuminated by 110,000 small ($M=1$ to $M=4$) earthquakes, including both background seismicity and aftershock swarms from larger events. When viewed in 3-D, it becomes clear that the seismicity is dominated by a major sub-horizontal band of events at about 10-15 km depth. The zone steepens below eastern Taiwan to 30° – 90° and reaches depths of 30–60 km. We interpreted this feature as the Main Detachment of the mountain belt. Other planes of seismicity above and below abut against this detachment, indicating its through-going nature. Although the availability of focal mechanisms is limited because of the small size of most earthquakes, the available mechanisms consistently show oblique slip with reverse component on the dipping part of the detachment. The imaged 3-D shape of the Main Detachment in relation to surface topography allows us a straightforward test of critical taper wedge mechanics and suggests that the first-order topography of Taiwan is controlled by the shape of the detachment. In fact, the reversal of topography at the crest of the mountain belt corresponds to the inflection of the Main Detachment under eastern Taiwan (fig. 4).

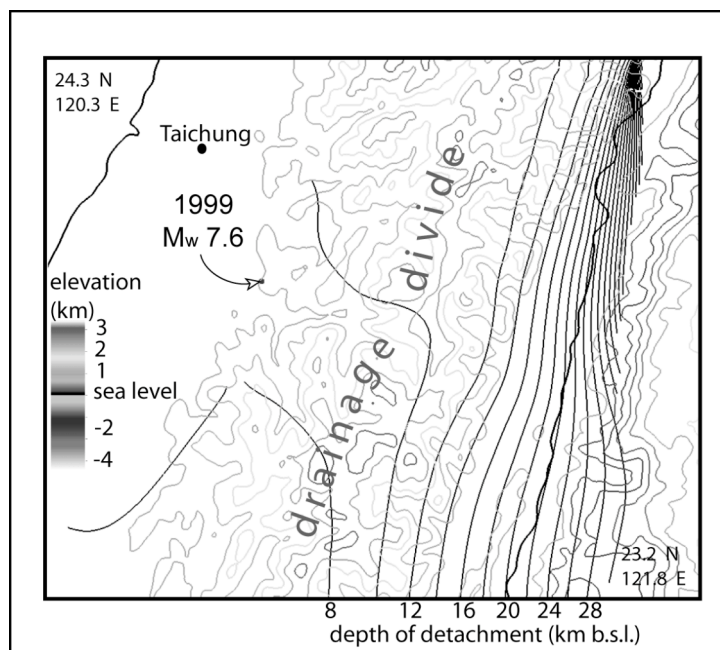


Fig. 4. Relationship between topography and the Main Detachment.

This geometry is consistent with critical-taper wedge mechanics (DAVIS ET AL. 1983), and in particular with homogeneous mechanical properties for the shallow brittle part of the wedge. The geometry of the detachment also indicates that it is very weak: the effective coefficient of friction on the detachment itself (μ_b^*) that fits the data is 0.08 (CARENA ET AL. 2002). Some of the most dangerous faults that break the surface, like the Chelungpu thrust, are connected to the Main Detachment at depth (YUE ET AL. 2005).

3 Acknowledgments

I am grateful to Honn Kao and Robert Jones for their help with earthquake clustering. Many thanks also to Tony Dahlen for constructive discussion about critical taper wedge mechanics, and to John Suppe for the many insightful suggestions.

The original earthquake catalog data used in this work are from the Southern California Earthquake Center (SCEC), and from the Taiwan Central Weather Bureau (CWB).

4 References

- ALLEN, C.R. (1957): San Andreas fault zone in San Geronimo Pass, southern California. – *Geol. Soc. Am. Bull.*, 68: 315—350.
- CARENA, S., & SUPPE, J. (2002): Three-dimensional imaging of active structures using earthquake aftershocks: the Northridge thrust, California. – *J. Struct. Geol.*, 24: 887—904.
- CARENA, S., SUPPE, J., AND KAO, H. (2002): Active detachment of Taiwan illuminated by small earthquakes and its control of first-order topography. – *Geology*, 30 (10): 935—938.
- CARENA, S., SUPPE, J., AND KAO, H. (2004): Lack of continuity of the San Andreas fault in southern California: fault models and earthquake scenarios. – *J. Geophys. Res.*, 109, B04313, doi:10.1029/2003JB002643.
- DAVIS, D., SUPPE, J., AND DAHLEN, F.A. (1983): Mechanics of fold-and-thrust belts and accretionary wedges. – *J. Geophys. Res.*, 88: 1153—1172.
- ERSLEV, E.A. (1991): Trishear fault-propagation folding. – *Geology*, 19 (6): 617—620.
- GOT, J.L., FRECHERT, J., KLEIN, F.W. (1994): Deep fault plane geometry inferred from multiplet relative relocation beneath the south flank of Kilauea. – *J. Geophys. Res.*, 99: 15,375—15,386.
- JONES, R.H., & STEWART, R.C., 1997, A method for determining significant structures in a cloud of earthquakes. – *J. Geophys. Res.*, 102: 8245—8254.
- KIKUCHI M.; YAGI Y.; AND YAMANAKA Y. (2000): Source Process of Chi-Chi, Taiwan Earthquake of September 21, 1999 Inferred from Teleseismic Body waves. – *Bull. Earthq. Res. Inst. Univ. Tokyo*, 75:1—13.
- KING, G.C.P., STEIN, R.S., AND LIN, J. (1994): Static stress changes and the triggering of earthquakes. – In: LANGSTON, C.A. (Ed.): *The 1992 Landers, California, earthquake sequence*. – *Bull. Seismol. Soc. Am.*, 84 (3): 935—953.
- LEE, S.-J., & MA, K.-F. (2000): Rupture process of the 1999 Chi-Chi, Taiwan, earthquake from the inversion of Teleseismic data. – *Terrestrial, Atmospheric and Oceanic Sciences*, 11 (3): 591—608.
- LIU, J., SIEH, K., AND HAUKSSON, E. (2003), A structural interpretation of the aftershock "cloud" of the 1992 Mw7.3 Landers, California, earthquake. – *Seism. Soc. Am. Bull.*, 93: 1333 — 1344.
- MALLET, J.L. (2002): *Geomodeling*. New York, Oxford University Press: 624 p.
- MALLET, J.L., MASSOT, J., AND COGNOT, R. (1999): Fault characterization. – *Proceedings of the 19th Gocad Meeting*, Nancy School of Geology, Nancy, France, June 14-17, 1999. ASGA (Association Scientifique pour la Géologie et ses Applications).
- MEADE, B., HAGER, B., AND KING R. (2002): Block models of present day deformation in southern California constrained by geodetic measurements – *Eos Trans. AGU*, 83 (47), Fall Meet. Suppl., Abstract T62F-05.
- NICHOLSON, T., SAMBRIDGE, M., AND GUDMUNDSSON, O. (2000): On entropy and clustering in earthquake hypocentre distributions. – *Geophys. J. Int.*, 14: 37—51.
- RICHARDS-DINGER, K., & SHEARER, P.M.. (2000): Earthquake Locations in Southern California Obtained Using Source Specific Station Terms. – *J. Geophys. Res.* 105 (5): 10939—10960.

- RUBIN, A.M., GILLARD, D., AND GOT, J.L. (1999): Streaks of microearthquakes along creeping faults. – *Nature*, 400: 635–641.
- SHAW, J.H., PLESCH, A., DOLAN, J.F., PRATT, T.L., AND FIORE, F. (2002): Puente Hills blind-thrust system, Los Angeles, California. – *Bull. Seismol. Soc. Am.*, 92 (8): 2946–2960.
- SHAW, J.H., SHEARER, P.M. (1999): An elusive blind-thrust fault beneath metropolitan Los Angeles. – *Science*, 283: 1516–1518.
- SUPPE, J. (1983): Geometry and kinematics of fault-bend folding. – *Am. J. Sci.*, 283: 684–721.
- THIBAUT, M., GRATIER, J.P., LEGER, M., MORVAN, J.M. (1996): An inverse method for determining three-dimensional fault geometry with thread criterion: application to strike-slip and thrust faults (Western Alps and California). – *J. Struct. Geol.*, 18: 1127–1138.
- WALDHAUSER, F., AND ELLSWORTH, W.L. (2002): Fault structure and mechanics of the Hayward Fault, California, from double-difference earthquake locations. – *J. Geophys. Res.*, 107: doi:10.1029/2000JB000084.
- YUE, L.-F., SUPPE, J., AND HUNG, J.-H. (2005): Structural geology of a classic thrust belt earthquake: the 1999 Chi-Chi earthquake Taiwan (Mw = 7.6). – *J. Struct. Geol.*, 27 (11): 2058–2083.
- YULE, D., & SIEH, K. (2001): The paleoseismic record at Burro Flats: evidence for a 300-year average recurrence for large earthquakes on the San Andreas fault in San Geronio Pass, southern California. – GSA Cordilleran Section 97th Annual Meeting, and Pacific Section AAPG, Universal City, CA, 2001.
- YULE, D., & SIEH, K. (2003): Complexities of the San Andreas Fault near San Geronio Pass: implications for large earthquakes. – *J. Geophys. Res.*, 108 (11): 2584, doi:10.1029/2001JB000451.